The Journal of Immunology

# Sialylation of 3-Methylcholanthrene–Induced Fibrosarcoma Determines Antitumor Immune Responses during Immunoediting

Merav Cohen, Moshe Elkabets, Michal Perlmutter, Angel Porgador, Elena Voronov, Ron N. Apte and Rachel G. Lichtenstein



*J Immunol* 2010; 185:5869-5878; Prepublished online 18 October 2010;
doi: 10.4049/jimmunol.1001635
http://www.jimmunol.org/content/185/10/5869



*The Journal of Immunology* is published twice each month by
The American Association of Immunologists, Inc.,
9650 Rockville Pike, Bethesda, MD 20814-3994.

Print ISSN: 0022-1767 Online ISSN: 1550-6606.

# Sialylation of 3-Methylcholanthrene–Induced Fibrosarcoma Determines Antitumor Immune Responses during Immunoediting

**Merav Cohen,*[,1] Moshe Elkabets,[†,1] Michal Perlmutter,* Angel Porgador,[†] Elena Voronov,[†] Ron N. Apte,[†] and Rachel G. Lichtenstein***

**Sialylation of tumor cells is involved in various aspects of their malignancy (proliferation, motility, invasion, and metastasis); however, its effect on the process of immunoediting that affects tumor cell immunogenicity has not been studied. We have shown that in mice with impaired immunoediting, such as in IL-1α$^{-/-}$ and IFNγ$^{-/-}$ mice, 3-methylcholanthrene–induced fibrosarcoma cells are immunogenic and concomitantly bear low levels of surface sialylation, whereas tumor cells derived from wild type mice are nonimmunogenic and bear higher levels of surface sialylation. To study immune mechanisms whose interaction with tumor cells involves surface sialic acid residues, we used highly sialylated 3-methylcholanthrene–induced nonimmunogenic fibrosarcoma cell lines from wild type mice, which were treated with sialidase to mimic immunogenic tumor cell variants. In vivo and in vitro experiments revealed that desialylation of tumor cells reduced their growth and induced cytotoxicity by NK cells. Moreover, sialidase-treated tumor cells better activated NK cells for IFN-γ secretion. The NKG2D-activating receptor on NK cells was shown to be involved in interactions with desialylated ligands on tumor cells, the nature of which is still not known. Thus, the degree of sialylation on tumor cells, which is selected during the process of immunoediting, has possibly evolved as an important mechanism of tumor cells with low intrinsic immunogenicity or select for tumor cells that can evade the immune system or subvert its function. When immunoediting is impaired, such as in IFN-γ$^{-/-}$ and IL-1α$^{-/-}$ mice, the overt tumor consists of desialylayed tumor cells that interact better with immunosurveillance cells.** ***The Journal of Immunology*****, 2010, 185: 5869–5878.**

Sialic acid, an acidic sugar at physiologic conditions that is found mainly at the outer ends of cell surface glycan chains, is elevated and frequently varied in glycan epitopes. In the malignant process, the presence of sialic acid is correlated with tumor cell proliferation, cell motility, invasion, metastasis, and poor prognosis (1–5). Studies addressing the effects of sialic acid on either tumor cell lipids or glycoproteins in modulating tumor-immune responses have shown that sialic acids can prevent cell–cell interactions, through nonspecific charge repulsion effects (6), participate in engagement of immune cell adhesion molecules such as the Ig-like lectin receptors (siglecs) (7, 8), and mask the underlying glycan structure, thus avoiding recognition by other lectins such as galectins and C-type lectins (9–11). Although the effects of sialylated tumor glycomolecules on immune responses have been examined (6–11), there is no information on levels of surface sialylation of selected tumor cells during tumor immunoediting and creating the immunogenic repertoire of malignant cells during tumorigenesis.

Several studies have experimentally proved the concept of immunoediting, in which immune responses of the host during tumorigenesis select tumor cell variants lacking stress ligands, Ags essential for immune recognition by immune effector cells, or tumor cells that can evade the immune system or subvert it (12–15). The immunoediting concept evolved from observations that tumors arising in immunodeficient mice present an immunogenic phenotype (16, 17). We have shown previously that tumors induced by the carcinogen 3-methylcholanthrene (MCA) in IL-1α–deficient mice were not properly edited and were thus highly immunogenic and nontumorigenic in intact mice, as compared with MCA-induced fibrosarcoma cells derived from wild type (WT) BALB/c mice (18). Surface sialylation levels and expression patterns of α2-6 sialyltransferase were lower in cell lines derived from IL-1α$^{-/-}$ mice than in cell lines derived from WT mice (19). This finding was also shown to be valid for cell lines derived from MCA-induced fibrosarcoma cells from IFN-γ$^{-/-}$ mice, because IFN-γ is a key component of the cancer immunoediting process (20). Because these immunodeficient cell lines bear low sialylation levels, we hypothesized that there is selection for tumor cell variants enriched in surface sialylation when immunoediting is intact. Variants arising from impaired immunoediting contain less sialylated surface glycoconjugates, which enables them to be immunogenic and less tumorigenic. Previously, we and others have also shown that innate immunosurveillance cells, especially NK cells, are involved in eradicating immunogenic tumor cell variants during the process of immunoediting both in IL-1α$^{-/-}$ and IFN-γ$^{-/-}$ mice, which subsequently shapes the immunogenic repertoire of the malignant cells (18, 20). NK cells play a major role in tumor immunosurveillance

*Department of Biotechnology Engineering, Faculty of Engineering; and [†]Shraga Segal Department of Microbiology and Immunology, Faculty of Health Sciences and National Institute of Biotechnology, Ben-Gurion University of the Negev, Beer-Sheva, Israel

[1]M.C. and M.E. contributed equally to this work.

Received for publication May 18, 2010. Accepted for publication September 17, 2010.

This work was supported by the Israel Glycobiology Center at Ben-Gurion University. R.G.L. is supported by the European Union Sixth Research Framework Programme (FP6). M.E. is supported by the International Sephardic Education Foundation and a Nehemia-Lev-Zion scholarship.

Address correspondence and reprint requests to Rachel G. Lichtenstein, Department of Biotechnology Engineering, Faculty of Engineering, Ben-Gurion University of the Negev, Beer-Sheva, 84105, Israel. E-mail address: ruha@bgu.ac.il

The online version of this article contains supplemental material.

Abbreviations used in this paper: FSG, fish gelatin; i.f.p., intrafootpad; MCA, 3-methylcholanthrene; MFI, mean fluorescence intensity; SNA, sambucus nigra lectin; T-Ag, Galβ(1,3)GalNAcα-1; Tn-Ag, GalNAcα-1; WT, wild type.



www.jimmunol.org/cgi/doi/10.4049/jimmunol.1001635

by serving as the first line of antitumor immune defense (21). The antitumor activity of NK cells is determined by a balance between stimulatory and inhibitory receptor signals, such as NKG2D and MHC class I molecules, respectively (22, 23). The abundant NKG2D ligands expressed on tumor cells better engage the activating NKG2D receptor, thus promoting NK-derived IFN-γ production. IFN-γ can activate various types of innate and adaptive immune mechanisms and enhance tumor cell lysis (24–26).

In this study, we have used an experimental model consisting of sialidase-treated cells derived from MCA-treated WT mice to assess the involvement of sialic acid residues in interactions of tumor cells with the host immune system. In a set of in vivo and in vitro experiments, we illustrate that the treated fibrosarcoma cells increased their immunogenic capacity and interactions with the host NK cells. Our in vivo experiments clearly show the involvement of NK cells in growth inhibition and lysis of low sialylated tumor cells. Our studies revealed a correlation between sialic acid expression levels on tumor cells, NKG2D ligand receptor engagement, and NK cell cytotoxic activity. NKG2D was found to be crucial in low-sialylated tumor cell lysis. The therapeutic potential of the results is discussed below.

## Materials and Methods

### *Mice*

Female BALB/c mice (6–14 wk old) were purchased from Harlan Breeders (Livermore, CA), and IFN-γ knockout mice were purchased from The Jackson Laboratory (Bar Harbor, ME). The generation of IL-1α$^{-/-}$ mice was described previously (27). These mice were backcrossed with BALB/c mice for more than eight generations and were homozygous for the relevant mutation. The mice were bred and kept at the Animal Facilities of the Faculty of Health Sciences, Ben-Gurion University, under aseptic conditions. Mice were treated according to the National Institutes of Health Animal Care guidelines adopted by the Ben-Gurion University Committee for the Ethical Care and Use of Animals in Research.

### *Cell lines and primary fibroblasts*

Fibrosarcoma cell lines were generated by injection of MCA (Sigma-Aldrich, St. Louis, MO), as previously described (28). Primary fibroblasts were produced from the dorsal skin of BALB/c and IL-1α$^{-/-}$ mice, as described previously (29). The cells were grown in DMEM (Invitrogen, Carlsbad, CA) supplemented with 10% (v/v) FCS, 100 U/ml penicillin, 0.1 mg/ml streptomycin, and 2 mM L-glutamine, in a humidified 5% $CO_2$ atmosphere at 37°C. All medium ingredients were purchased from Biological Industries (Bet-Haemek, Israel).

### *Sialidase treatment and kinetic analysis of sialic acid recovery*

For external reduction of terminal sialic acids, $6 \times 10^6$ cells were treated with 10 mU sialidase A (ProZyme, San Leandro, CA). Treatment was performed in 100 μl sodium-phosphate buffer (pH 6) for 10, 30, 45, and 60 min at 37°C. For kinetic analysis of the recovery of sialic acid residues after 1 h of treatment, $5 \times 10^5$ sialidase-treated cells were recultured in six-well plates in 2 ml medium. Cells were then harvested by trypsin-EDTA treatment at different points over 48 h. After multiple washes with PBS, the cells were fluorescently labeled with sambucus nigra lectin (SNA)-FITC lectin (Vector Laboratories, Burlingame, CA) for determination of α2-6 sialic acid levels by FACS. Recovery was calculated as the sialic acid level detected at a specific time, relative to the sialic acid level of fluorescently marked untreated cells of the same type (i.e., the basal level). Tumor cells treated for 1 h with sialidase were used in all experiments, except those showing the effects of gradient sialic acid levels.

### *Proliferation, apoptosis, and soft agar colony formation*

For proliferation analysis, $5 \times 10^3$ cells were seeded in 96-well plates in a volume of 200 μl and assessed by an assay based on WST-1 reagent (Roche, Mannheim, Germany), following the manufacturer's instructions. An apoptosis assay using an annexin V kit (Bender MedSystems, Burlingame, CA) was performed on $5 \times 10^5$ cells before and after sialidase treatment, followed by FACS analysis. Soft agar colony formation using sialidase-treated and untreated cells was assessed as described previously (30).

### *Fluorescence microscopy*

Cells ($1 \times 10^4$) were fixed in 4% formaldehyde in PBS for 15 min at room temperature, washed with PBS, and blocked with 1% fish gelatin (FSG) in PBS-Tween solution for an additional 30 min. Next, FITC-labeled SNA lectin (2.5 ng per sample) in PBS containing 0.2% FSG was added for 1 h at room temperature and then washed three times. Fluorescent staining of actin filaments was observed following labeling by (1:500) Oregon Green 488 phalloidin (Invitrogen) in PBS containing 0.2% FSG. For nuclear staining, (1:1000) Hoechst dye (Invitrogen) in PBS containing 0.2% FSG was added. Finally, all cover slips were placed on slides containing 50% glycerol and inspected with an inverted microscope equipped with an Olympus IX81 camera, using appropriate fluorescent filters (Olympus, Center Valley, PA).

### *Invasiveness of 3-MCA–induced cell lines*

For determining tumorigenicity patterns of sialidase-treated and untreated MCA-induced fibrosarcoma cells, $1 \times 10^5$ cells were suspended in 50 μl PBS and injected intrafootpad (i.f.p.) in control or irradiated BALB/c mice (5 Gy of γ-Cobalt 60 per mouse; i.e., 600 rad). Local tumor growth was determined every 2–3 d by caliper measurement of tumor diameter.

### *Metastasis of MCA-induced cell lines*

For determining lung metastasis, sialidase-treated and untreated cells ($1 \times 10^6$) were suspended in 200 μl PBS and injected i.v. into the tail vein of mice. Two weeks later, mice were sacrificed and their lungs were weighed and photographed with a digital camera. Mouse survival was determined daily during the 40 d after i.v injection.

### *Spleen cell isolation and NK cell enrichment*

Spleen cells derived from mice were cultured in 24-well plates at a concentration of $1 \times 10^6$ cells per well. Splenic NK cell were enriched using a negative selection kit, according to the manufacturer's instructions (Miltenyi Biotec, Bergisch Gladbach, Germany). NK cell enrichment was verified by FACS analysis. Approximately 75–90% of the recovered cells were CD3$^-$DX5$^+$ CD122$^+$.

### *Coculturing of tumors with immune cells and NKG2D ligand blocking*

MCA-induced fibrosarcoma cells treated with mitomycin-C (Sigma-Aldrich; 100 μg/$10^7$ cells treated for 1 h at 37°C) were added to naive spleen or enriched NK cells, as described previously (24). Cocultures were incubated in RPMI 1640 medium (Invitrogen) supplemented with 10% FCS, 2 mM L-glutamine, 100 u/ml penicillin, 0.1 mg/ml streptomycin, and 100 ng/ml IL-2. Coculture supernatants were collected 24 h after seeding, and cytokine amounts in the culture supernatants were measured by ELISA. To quantify secreted IFN-γ in cocultures with a blocked NKG2D receptor, $1 \times 10^6$ enriched NK cells were preblocked with 0.5 μg anti-NKG2D/CD134 Abs (eBioscience, San Diego, CA) in a volume of 100 μl for 30 min at 4°C. The treated NK cells were cocultured with sialidase-treated or untreated cells after supernatant collection and cytokine assessment by ELISA.

### *Intracellular staining*

For intracellular IFN-γ detection, cocultures were supplemented with 100 ng/ml IL-12, followed by Golgi-stop treatment (BD Biosciences, San Jose, CA) using a diluted stock solution of 1:1000 12 h later, and stained using a Cytofix/Cytoperm kit according to the manufacturer's instructions (BD Pharmingen, San Diego, CA). The cells were finally stained with NK cell markers and anti–IFN-γ Abs and subsequently quantified by FACS analysis.

### *NKG2D-Ig ligand binding*

For detection of NKG2D ligands by flow cytometry, cell lines were stained with an mNKG2D-fusion protein (mNKG2D-FP) (31). For kinetic measurements of NKG2D ligand–receptor interactions, $6 \times 10^6$ untreated fibrosarcoma cells were preincubated with 10 mU sialidase every 10 min for 1 h. The treated cells were washed with PBS and then incubated with mNKG2D receptor-fusion protein (mNKG2D), as described previously (30).

### *In vivo depletion of lymphoid cell subpopulations*

In vivo depletion of CD4$^+$ and CD8$^+$ T cells was achieved via multiple i.p. injections of ascitic fluids containing the relevant monoclonal Abs—GK1.5 and YTS-169, respectively. Injection of Abs was performed on days

−5, −3, and −1 before injection of tumor cells ($1 \times 10^5$ cells per mouse i.p.f. or $1 \times 106$ cells per mouse, i.v.) and twice per week thereafter. For in vivo NK depletion, mice were inoculated i.p. with 0.2 ml anti-asialo GM1 rabbit serum (Wako BioProducts, Richmond, VA; 1:10 dilution in PBS). Anti-asialo GM1 rabbit serum was administered to mice on days −3, −1, and +1 after tumor cell inoculation and then every 5 d. Depletion of specific lymphoid cells in the spleen was verified by FACS analysis.

### *Flow cytometry*

To detect surface α2-6 sialic acids on primary and tumor cells, skin fibroblasts and MCA-induced tumor cell lines were stained with FITC-labeled SNA lectin, as described previously (25). For detection of MHC class I and NKG2D ligands, the cell lines were harvested and blocked with PBS plus 0.5% FBS and purified anti-CD16/CD32 Abs (Biolegend, San Diego, CA). Subsequently, the cells were stained with MHC class I-FITC–conjugated mouse anti–H-$2K^d$ mAbs (clone SF1-1.1; BD Pharmingen) and mNKG2D-FP. Biotinylated donkey anti-human IgG antiserum (Jackson ImmunoResearch Laboratories, West Grove, PA) was used as a second-step reagent, followed by staining with PE-conjugated streptavidin (Jackson ImmunoResearch Laboratories).

Isolated spleen cells from BALB/c mice were stained for cell subsets by APC-PE–labeled anti-CD49b (clone DX5; Biolegend), anti-mouse CD122-PE (BD Biosciences), FITC–anti-mouse CD3ε (Biolegend), and ALEXA647–anti-mouse NKP46 (eBioscience) Abs.

### *Frozen and paraffin section analysis*

Tumors were removed from the footpads or lungs of mice injected with sialidase-treated or untreated tumor cells. For paraffin sections, the tumors were immediately fixed and stained with H&E using an established protocol (27). For frozen sections, tumors were fixed and stained as described previously (32). Paraffin or frozen stained sections were viewed with light or confocal microscopes at ×20 and ×40 magnification, respectively.

### *Measurement of secreted cytokines*

Murine IFN-γ, TNF-α, IL-2, IL-4, IL-6, and IL-12 levels were measured using a commercial ELISA kit (BD Pharmingen), according to the manufacturer's instructions and as described previously (33).

### *Cytolytic assay*

For in vitro and in vivo NK cell cytolytic activity assays, 200 μg of poly(I):poly(C) (Sigma-Aldrich) were injected into naive mice, and spleen cells were removed 18 h later (34). The cytolytic activity was evaluated in cocultures of target cells with the treated spleen cells in a 4-h CFSE/7-AAD flow cytometry assay as described (35). For in vivo NK cell-killing assays (34), sialidase-treated cells were labeled with the fluorescent dye Vybrant Dil (Invitrogen), and untreated cells were labeled with the fluorescent dye Vybrant DiD (Invitrogen). Cells were mixed at a density of $2 \times 10^7$ cells of each population per milliliter of PBS, and 200 μl was injected into the tail vein. Lungs were collected after the injections or 5 h later, single-cell suspensions were obtained with cell strainers, and fluorescence was analyzed by flow cytometry. The ratio of treated target cells to untreated cells was calculated. For in vivo NK cell killing after NKG2D blocking, mice were injected i.p. with 200 μg anti-NKG2D/CD134 Abs per mouse, 24 h before injection of sialidase-treated and untreated tumor cells.

### *Cell conjugation and confocal analysis*

To evaluate the number of immune synapses formed by NK and target cells, poly(I):poly(C) activated NK cells were isolated from naive mice and conjugated to sialidase-treated or untreated fibrosarcoma cells at a ratio of 2:1 on poly-L-lysine–coated glass slide chambers (Sigma-Aldrich). Adherent cells were fixed, permeabilized, and washed using the Cytofix/Cytoperm kit (BD Biosciences). Staining NK and tumor cell conjugates with anti-mouse CD11a Abs (clone M17/4; Biolegend) was followed by staining with Alexa Fluor 633-conjugated anti-rat IgG (Invitrogen) for LFA-1 detection. To detect F-actin, cells were stained with Oregon green 488 phalloidin (Invitrogen). VECTASHIELD Mounting Medium (Vector Laboratories) with DAPI was subsequently added to stain nuclei and preserve fluorescent intensity. The cell conjugates were viewed in a Zeiss Laser Scanning Confocal Microscope (Goettingen, Germany). Each conjugate was scored for polarization of the activating synapse markers LFA-1 and F-actin, as described previously (36). Synapse formation percentages were calculated by dividing the number of conjugates showing polarization of activating synapse markers to the total number of conjugates.

### *Statistical analysis*

Each experiment was repeated at least three times with similar response patterns. In experiments on the invasiveness of MCA-induced fibrosarcoma cell lines, experimental groups consisted of 5–10 mice. The data shown correspond to pooled or single representative experiments, as indicated, and are expressed as mean ± SD. Significant differences in results were determined using the two-sided Student $t$ test, with $p < 0.05$ being considered significant.

## Results

### *Surface sialylation levels of MCA fibrosarcomas derived from immunodeficient or BALB/c mice are slowly recovered after sialidase treatment*

We first documented the natural level of sialic acids in MCA fibrosarcomas derived from WT mice. The sialic acid levels were compared with those inspected in immunogenic fibrosarcoma cell lines originating from IL-$1\alpha^{-/-}$ mice (19), as well as in primary fibroblasts, by fluorescence microscopy and flow cytometry using FITC-tagged SNA, which is able to bind α2-6 sialic acid. Whereas primary fibroblasts derived from WT and IL-$1\alpha^{-/-}$ mice showed similar staining with SNA (Fig. 1*A*), MCA-induced fibrosarcoma cell lines derived from IL-$1\alpha^{-/-}$ mice exhibited low staining and binding with SNA, as compared with fibrosarcoma cell lines derived from WT mice (Fig. 1*A*). These results coincide with flow cytometry evaluations of sialic acid levels in additional MCA-induced fibrosarcoma cell lines originated from IFN-$\gamma^{-/-}$ mice in our laboratory (Fig. 1*B*). Mice lacking IFN-γ have been shown to bear increased susceptibility to MCA-induced sarcoma (20). As such, sarcoma immunogenicity in the second recipients was confirmed in our IFN-$\gamma^{-/-}$ cell lines. As expected, IFN-$\gamma^{-/-}$ cells injected i.f.p. developed tumors at a lower rate than did WT fibrosarcomas (Fig. 1*B*). Collectively, these results indicate that sialic acid surface expression is elevated during carcinogenesis and is associated with tumor immunoediting.

Fibrosarcoma cell lines derived from WT mice were treated with sialidase A, which cleaves nonreducing terminal sialic acid in α2, α3, α6, α8, or v9 linkages and which are stained by SNA (Supplemental Fig. 1*A*). The renewal of sialic acid levels to the original status was examined in sialidase-treated WT and IL-$1\alpha^{-/-}$ fibrosarcoma cell lines. According to our previous study, MCA-induced fibrosarcoma cell lines derived from IL-$1\alpha^{-/-}$ mice express lower amounts of α2-6 sialyltransferase (ST6GalI) compared with fibrosarcoma cells derived from naive BALB/c mice (19). Therefore, the recovery of sialic acids on IL-$1\alpha^{-/-}$ tumor cells was also 50% lower than sialic acid recovery on fibrosarcoma cell lines derived from BALB/c mice at the same time (Supplemental Fig. 1*B*). Complete recovery of sialic acid levels was obtained after ∼48 h, a period that allows in vivo examination of the immune response of the sialidase-treated tumor cells.

To verify that cellular competency was not impaired by the sialidase treatment, the rates of proliferation, the ratio of apoptosis, and the ability of the cells to form colonies on soft agar were assessed. No significant differences in proliferative ability, colony formation, or apoptotic ratios were observed between the sialidase-treated and untreated cells. These results indicate that siladiase-treated cells can be used as a model for studying the role of tumor cell sialylation in antitumor immunity in vivo (Fig. 1*C*).

### *Host response to sialidase-treated tumor cells results in tumor growth inhibition*

We next studied the in vivo contribution of desialylated fibrosarcoma cells to tumor progression. Injection of sialidase-treated tumor cells into the footpads of syngenic mice resulted in an

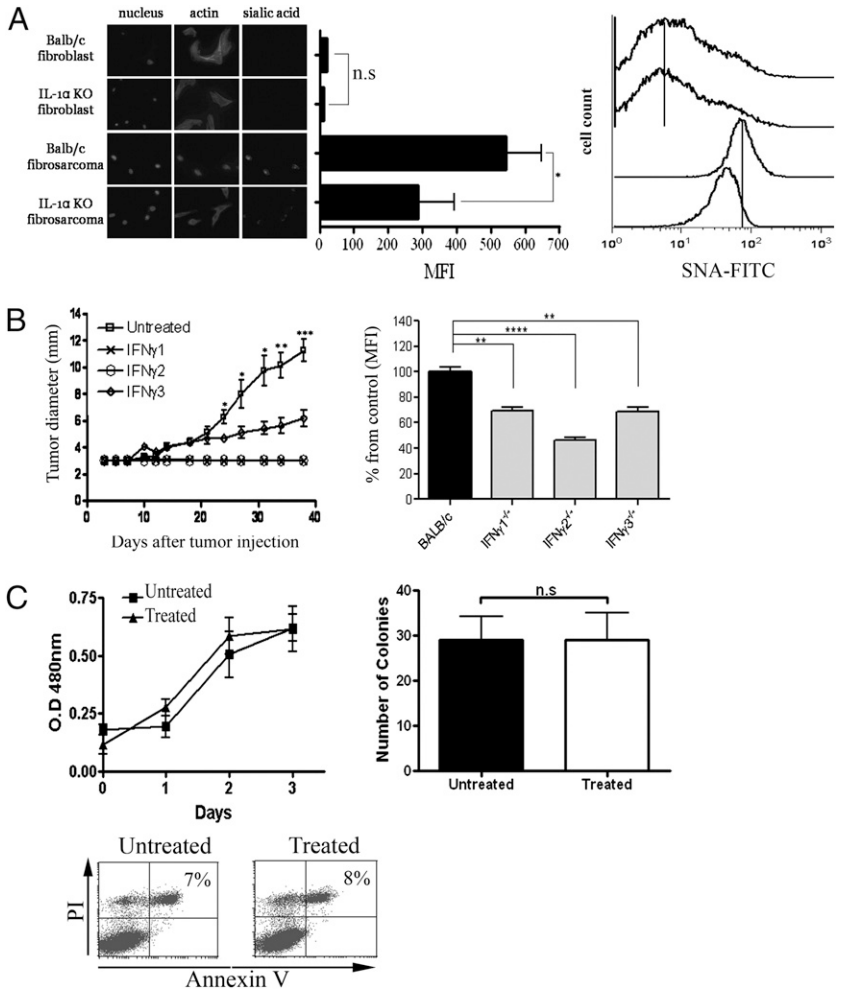


**FIGURE 1.** Surface sialylation levels of MCA fibrosarcomas derived from immunodeficient or BALB/c mice slowly recover after sialidase treatment, allowing for examination of in vivo immune response. Sialic acids on the surface of primary fibroblasts and MCA-induced fibrosarcoma cells derived from BALB/c and IL-1$\alpha^{-/-}$ mice were stained with SNA-FITC lectin and detected by fluorescence microscopy (mean fluorescence intensity [MFI]) and a flow cytometry (histogram) *A*, i.f.p injections of $2 \times 10^5$ fibrosarcoma cells derived from WT or IFN-$\gamma^{-/-}$ mice into naive BALB/c mice were followed by tumor diameter measurement (*B*, *left panel*). Surface sialic acids on MCA fibrosarcoma cells derived from WT (□) or IFN-$\gamma^{-/-}$ (○, ◊, ×) mice were stained with SNA-FITC lectin and analyzed by flow cytometry (*B*, *right panel*). The proliferation potency, apoptotic rate, and colony formation of sialidase-treated cells (▲) compared with untreated cells (■), were assessed using a WST-1 proliferation kit, annexin-propidium iodide, V-PI staining and a soft agar colony assay (*C*). Data represent the mean ± SD of duplicate or triplicate measurements from duplicate or triplicate independent experiments. $***p < 0.005$; $**p < 0.01$; $*p < 0.05$, versus the appropriate controls in each panel.

inhibition of tumor growth that lasted ~30–40 d after tumor cell injection, as compared with the rapid tumor growth rate observed with untreated cells (Fig. 2*A*). Similar injection of treated cells 0–60 min after sequential sialidase treatments resulted in a linear gradient of tumor growth inhibition (Supplemental Fig. 2*A*). In addition, i.v injection of sialidase-treated cells into mice resulted in 100% survival, compared with the earlier death of mice injected with untreated cells (Fig. 2*B*). Lung analysis performed 2 wk after untreated cell injection showed significantly high metastasis formation, as indicated by lung weights in mice injected with untreated cells, relative to lungs from mice injected with treated cells (Fig. 2*C*). Next, sialidase-treated and untreated tumor cells were injected i.f.p. and i.v. into immunocompromised, sublethally irradiated mice. The sialidase-treated and untreated tumor cells induced the formation of solid tumors, leading to similar kinetics of mouse death (Fig. 2*D*). These results indicate that sialidase-treated cells are likely to be immunogenic and did not lose their invasive potential.

Histologic section analysis of the i.f.p. injection site showed greater accumulation and migration of infiltrate cells within the first day of sialidase-treated cell injection, as compared with what was seen with injection of untreated cells. Ten days later, a solid tumor was detected at the site injected with untreated cells. A much smaller tumor was observed when sialidase-treated cells were injected (Fig. 2*E*). In lungs, micrometastasis was observed 14 d after i.v. injection with sialidase-treated cells, as compared with the macrometastasis seen with untreated tumor cells (Fig. 2*F*). These observations indicate that the low levels of sialic acid on malignant cells resulted in tumor growth inhibition and enhanced leukocyte migration into the tumor microenvironment.

### *NK cells are involved in tumor growth inhibition of sialidase-treated cells*

Identifying the lymphoid cell subsets involved in tumor inhibition of sialidase-treated cells was achieved by in vivo assessment of tumor growth in NK or T cell-depleted mice (Supplemental Fig. 2*B*). Depletion of $CD4^+$ and $CD8^+$ T cells resulted in similar kinetics of sialidase-treated tumor growth inhibition following i.f.p. injection, as observed in intact mice. By contrast, NK cell depletion had the most significant effects on the growth of sialidase-treated tumor cells, as compared with growth in intact mice (Fig. 3*A*). Lung weights were significantly elevated in NK-depleted mice that were injected i.v. with sialidase-treated cells, as compared with lung weights measured in $CD4^+$-depleted, $CD8^+$-depleted, or WT mice injected with treated cells (Fig. 3*B*).

Further evidence pointing to the NK cell involvement in tumor inhibition of sialidase-treated cells was observed by immunohistochemical examination of frozen sections. Analysis of the i.f.p. injection site revealed significant accumulation and migration of NK cells in the infiltrate cells within 2 d after sialidase-treated cell injection (Fig. 3*C*).

Finally, the number of synapses was evaluated by conjugating activated NK cells to sialidase-treated or untreated cells. Immune synapses were quantified by determining the polarization of LFA-1 and F-actin at the interface between the effector and target cells. Anti-CD11a (LFA-1) Abs stained integrin molecules that participate

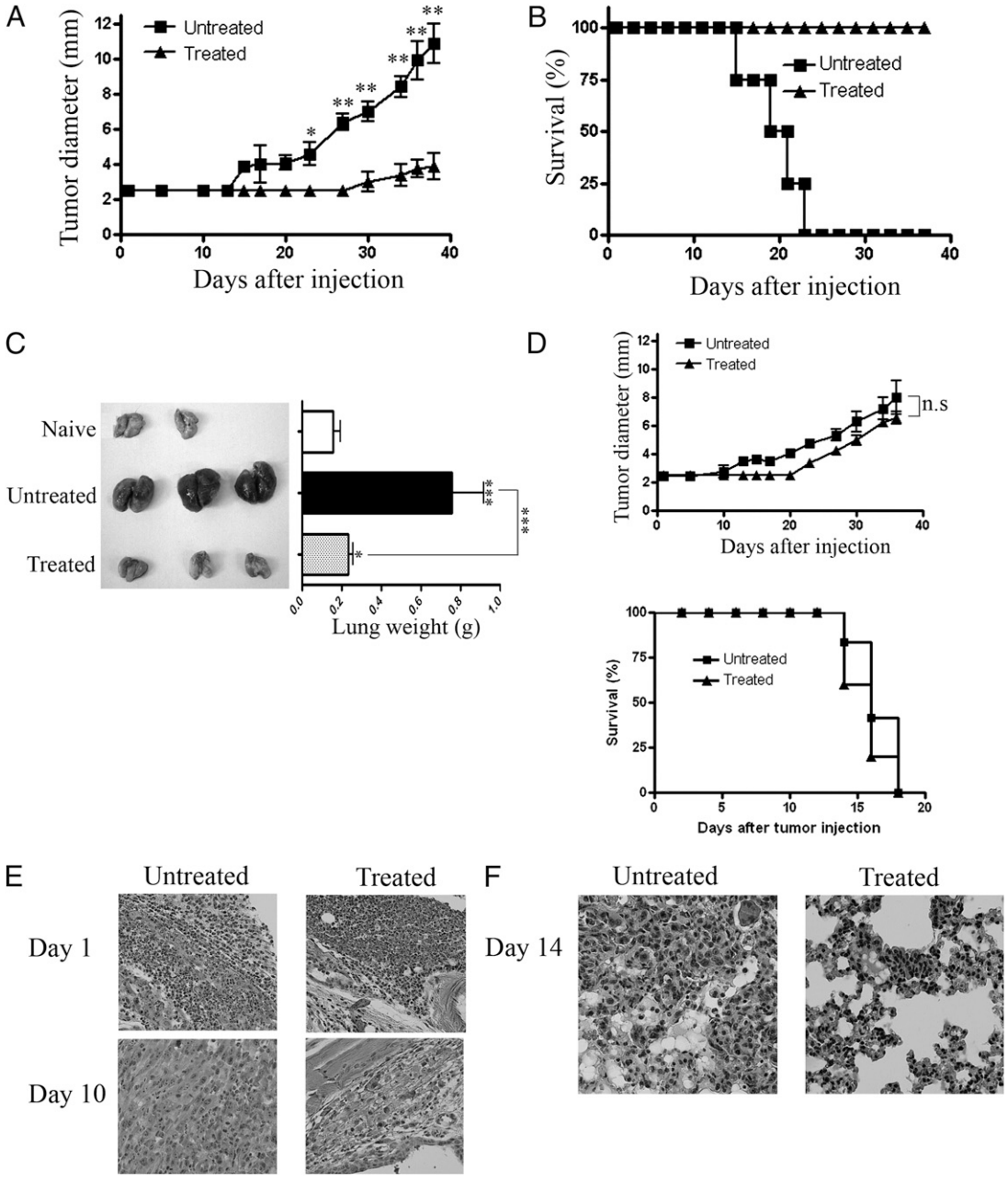


**FIGURE 2.** The host response against sialidase-treated tumor cells results in tumor growth inhibition is shown. *A*, Sialidase-treated (▲) or untreated (■) tumor cells ($2 \times 10^5$) were injected i.f.p. into naive BALB/c mice, and tumor diameters were measured. *B*, Sialidase-treated (▲) or untreated (■) tumor cells ($1 \times 10^6$) were injected i.v. into naive mice, and the mortality rate was recorded. *C*, Sialidase-treated or untreated tumor cells ($1 \times 10^6$) were injected i.v. into naive BALB/c mice, whereas 14 d later lungs were harvested and metastasis gross morphology and weight were measured. *D*, Tumor size and mortality rate were measured in irradiated BALB/c mice (5 Gy) injected i.f.p. or i.v. with $2 \times 10^5$ or $1 \times 10^6$ sialidase-treated (▲) and untreated cells (■), respectively. *E*, H&E staining of 4-μm footpad sections 1 and 10 d after injecting sialidase-treated or untreated cells into BALB/c mice. *F*, H&E staining of 4-μm lung sections 14 d after injecting sialidase-treated or untreated cells into BALB/c mice. Footpad and lung sections were viewed under light microscopy (original magnification, ×20). Tumor growth was examined every 2 or 3 d, and data are the means ± SE of four or five mice in each group. Each graph showing tumor invasiveness is representative of one fibrosarcoma cell line from two fibrosarcoma cell lines that were examined. Each experiment was repeated two or three times. $***p < 0.005$; $**p < 0.01$; $*p < 0.05$, versus the appropriate controls in each panel.

in the adhesion and stimulation of NK cells and their target cells. F-actin staining showed tight collars at the contact site owing to the accumulation of actin during formation of conjugates (Fig. 3*D*). There were 3-fold more immune synapses between NK cells and sialidase-treated cells compared with untreated cells. In some cases, a single NK cell was found to form simultaneous immune synapses with more than one sialidase-treated tumor cell. In contrast, fewer synapses were formed by highly sialylated tumor cells and NK cells. These data show the contribution of NK cells to sialidase-treated tumor cell inhibition in vivo and show the cytotoxic interactions between NK cells and sialidase-treated tumor cells in vitro.

### *Reduction of sialic acid levels triggers IFNγ secretion and NK cell cytotoxicity*

To further investigate the nature of the immune response against sialidase-treated cells, immune-secreted cytokines were assessed in vitro. Coculturing of sialidase-treated tumor cells with naive

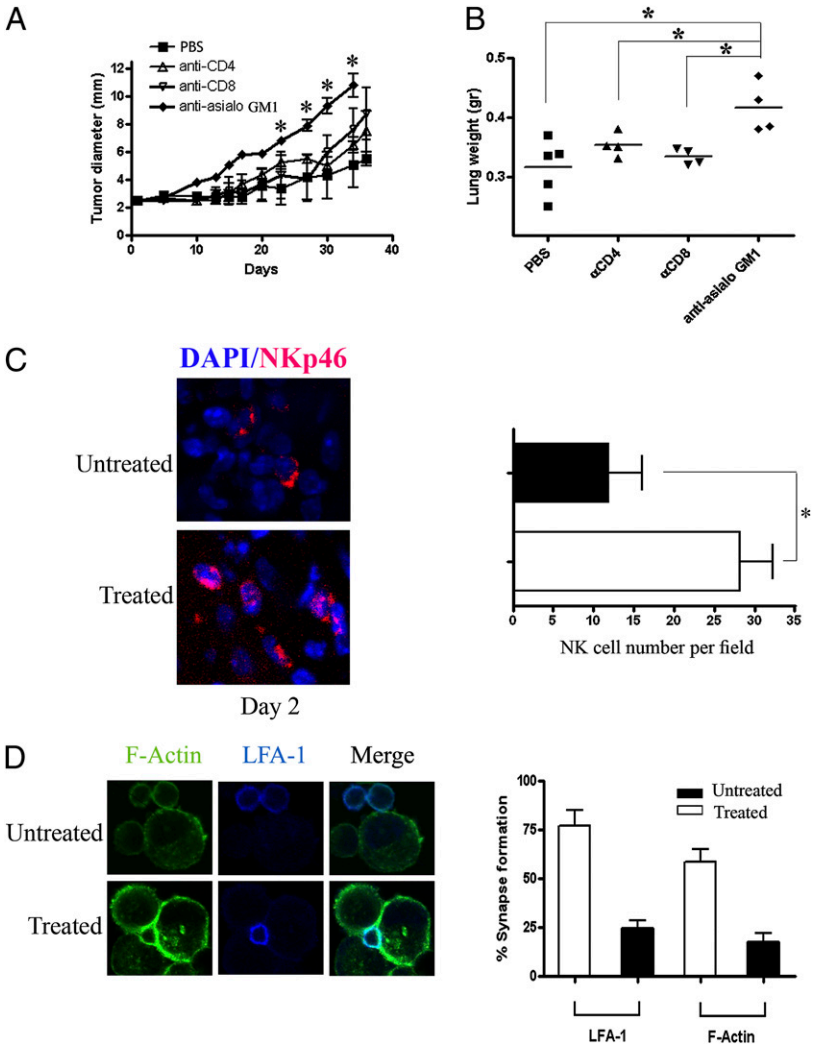


**FIGURE 3.** NK cells are involved in tumor growth inhibition of sialidase-treated cells. Depletion of CD4, CD8, and NK cells in BALB/c mice was achieved by multiple i.p. injections of PBS, anti-CD4, anti-CD8, and anti–asialo-GM1 Abs, respectively. *A*, Sialidase-treated cells ($2 \times 10^5$) were injected i.f.p. into the depleted mice and tumor diameters were measured. *B*, Sialidase-treated cells ($1 \times 10^6$) were injected i.v. into the depleted mice, and 35 d later the mice were sacrificed and lungs were weighed. *C*, Two days after i.f.p. injection of $2 \times 10^5$ sialiase-treated or untreated cells, 12-μm frozen sections of the injection site were stained by anti-NKp46 Alexa-647-conjugated Abs to detect NK cells and with DAPI to label cell nuclei. *D*, Immune synapses of activated NK cells and sialidase-treated or untreated cells were formed by merging LFA-1 in NK cells and F-actin staining. NK cells were stained by anti-CD11a Abs followed by Alexa Flour 633-conjugated goat anti-rat IgG and F-actin by Oregon green 488 phalloidin. The synapses were quantified by counting conjugates presenting polarization of LFA-1 and F-actin divided by the total number of conjugates (defined as two cells in contact). The synapses and sections containing NKp46-positive cells were examined under a Zeiss Laser Scanning Confocal Microscope (original magnification ×40). Synapses and NKp46-positive cells were counted in random fields. $^{**}p < 0.01$; $^{*}p < 0.05$, versus the appropriate controls in each panel.

spleen cells for 24 h resulted in an induction of IFN-γ secretion to a level 2-fold higher than that observed in response to untreated cells (Fig. 4*A*). Coculturing of tumor cells treated with sialidase for 30, 45, and 60 min inversely correlated with IFN-γ production (Fig. 4*B*). This finding was due to a 50%, 60%, and 75% gradient of sialic acids generated on the tumor cells. NK cell depletion reduced IFN-γ concentration by 50% in cocultures of spleen cells with sialidase-treated tumor cells, as compared with similar incubation with intact spleen cells (Fig. 4*C*). By contrast, similar IFN-γ concentrations were observed in untreated tumor cells cocultured with either NK-depleted or intact spleen cells, indicating that the NK cells are the major source of IFN-γ production when interacting with sialidase-treated cells. Likewise, TNF-α, IL-2, IL-4, IL-6, and IL-12 were not differentially secreted in response to coculturing with sialidase-treated or untreated tumor cells (data not shown). In addition, comparison of IFN-γ levels secreted by cocultures of the immunogenic IL-1α$^{-/-}$ tumor cells with naive spleen cells revealed increased IFN-γ secretion to a level 10- or 5-fold higher than observed in response to untreated cells (Supplemental Fig. 3) or treated cells, respectively, as shown in Fig. 4*A*. Most likely, IL-1α$^{-/-}$ tumor cells trigger more than one immune cell populations to produce IFN-γ, whereas sialidase-treated cells mainly trigger the NK cell population.

To confirm that IFN-γ is secreted by NK cells, intracellular staining of the various cocultures was performed, whereas naive spleen cells were stained for DX5$^+$ and CD3$^-$ to confirm expression of the NK cell marker NKp46 (Supplemental Fig. 4). As shown in Fig. 4*D*, IFN-γ accumulated in DX5$^+$CD3$^-$ cells from cultures containing sialidase-treated cells to twice the level seen in cultures containing untreated cells. Moreover, in cocultures of freshly isolated NK and sialidase-treated cells, IFN-γ accumulation increased by more than 2-fold, relative to levels in cocultures of freshly isolated NK and untreated cells (Fig. 4*E*).

Finally, the role of NK cells in the lysis of sialidase-treated cells was illustrated in vitro by addressing cocultures containing poly(I):poly(C) pretreated naive spleen cells and by in vivo i.v injections of a labeled sialidase-treated and untreated cell mixture. The coculturing results revealed 32% specific lysis of sialidase-treated cells, relative to the low percentages observed in untreated cells (Fig. 4*F*). In vivo lysis decreased from an initial ratio of 1.0 between treated to untreated cells after injection to a ratio of 0.71 after 1 h and to a ratio of 0.23 5 h later, indicating a rapid lysis of sialidase-treated cells compared with untreated cell lysis (Fig. 4*G*). These results reveal that poorly sialylated tumor cells are more susceptible to NK cells than are highly sialylated tumor cells.

### *Sialylation is involved in the binding of NKG2D ligands and affects subsequent IFN-γ secretion and NK cell cytotoxicity*

In certain conditions, stress-induced ligands, such as NKG2D ligands, induce NK cell activation and IFN-γ secretion. Because the involvement of tumor sialylation in NKG2D engagement and IFNγ secretion had not been characterized, we initially

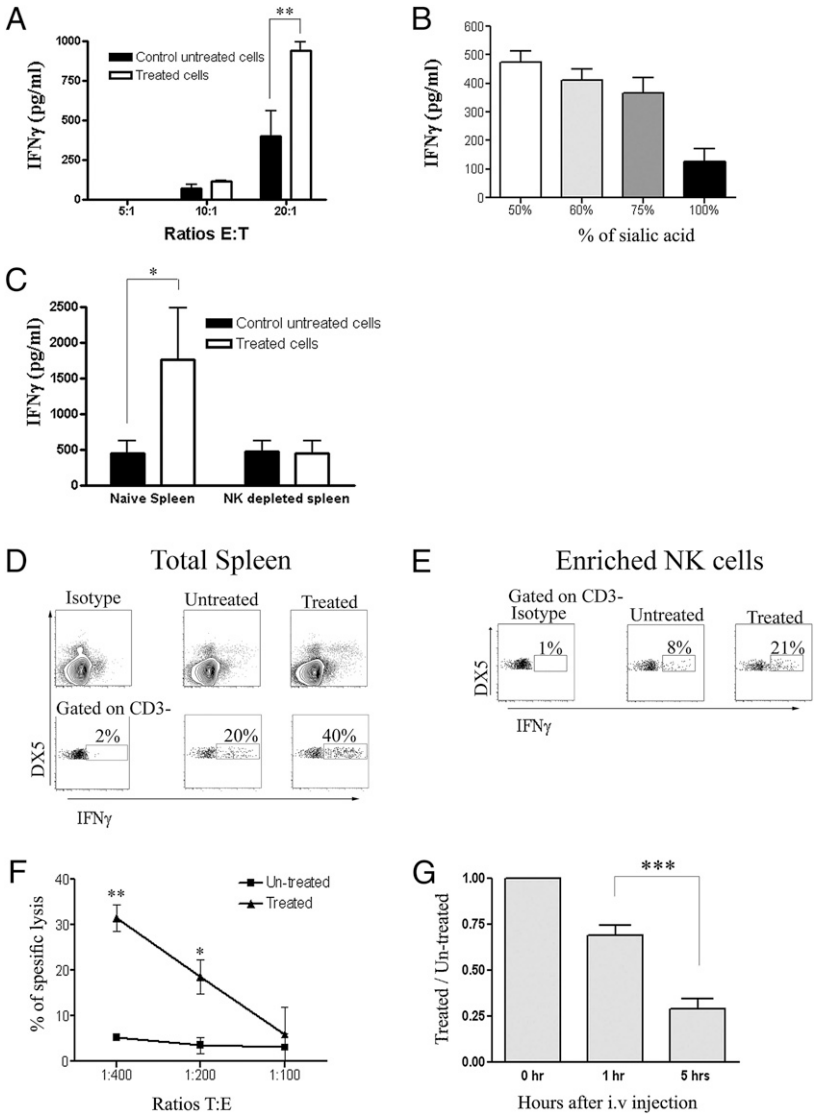


**FIGURE 4.** Reduction of sialic acid levels from MCA-induced fibrosarcoma cells triggers IFN-γ secretion and NK cell cytotoxicity. Supernatants of 24 h cocultures were collected, and IFN-γ levels were assessed by ELISA. *A*, The cocultures contained sialidase-treated or untreated tumor cells and naive spleen cells at different effector:target ratios. *B*, The cocultures contained untreated or sialidase-treated (for 30, 45, or 60 min) tumor cells and naive spleen cells or (*C*) sialidase-treated or untreated tumor cells and spleen cells derived from NK-depleted mice at different effector:target ratios. *D*, Intracellular staining of IFN-γ was assessed in cocultures of sialidase-treated or untreated tumor cells with naive spleen cells. The entire culture (*top*) or $CD3^-$-gated cells (*bottom*) were stained with anti-DX5 and anti–IFN-γ Abs. *E*, Freshly isolated NK cells were cocultured with sialidase-treated or untreated cells in the presence of IL-2 for 24 h, stained with anti-DX5 Abs, and perforated and stained with anti-IFNγ Abs to assess intracellular IFN-γ. *F*, Poly(I):poly(C)-treated spleen cells were labeled with CFSE then cocultured with treated (▲) or untreated (■) cells at different effector:target ratios. After 5 h incubation at 37°C, cells were stained with 7-aminoactinomycin D, and specific lysis was evaluated by counting viable cells relative to spontaneous lysis, by flow cytometry. *G*, Vybrant Dil-labeled sialidase-treated and Vybrant DiD-labeled untreated cells ($2 \times 10^7$) were mixed and injected into the tail veins of three naive BALB/c mice. Lungs were harvested and cells were quantified 0, 1, and 5 h after injection using flow cytometry. The ratio of treated target cells to untreated cells was calculated. Data represent the mean ± SD of duplicate or triplicate measurements from duplicate or triplicate independent experiments. In vivo experiments included 3 mice in each group. $^{**}p < 0.01$; $^{*}p < 0.05$, versus the appropriate controls in each panel.

assessed NKG2D ligand binding to an mNKG2D fusion protein. The dependency of NKG2D engagement on sialic acid expression was illustrated by kinetic experiments. MCA-induced fibrosarcoma cells derived from WT mice were treated with sialidase for 1 h. Every 10 min during the treatment, cells were assessed for sialic acid and MHC class I levels, using SNA lectin and anti-H-$2K^d$ Abs, respectively. Binding of the mNKG2D fusion protein increased with a decrease in SNA binding, whereas MHC class I binding to anti–H-$2K^d$ Abs did not change during the sialidase treatment (Fig. 5*A*). These findings show the effect of the sialylation level on the ability of tumor NKG2D ligands to be recognized by the NKG2D receptor (Fig. 5*B*).

Because the increase in binding capacity of NKG2D ligands is related to the ability of NK cells to produce IFN-γ or cytotoxic activity, we were interested in assessing these phenomena as a function of different levels of tumor sialylation. Accordingly, the NKG2D receptor was blocked by pretreatment of freshly isolated NK cells with anti-NKG2D/CD134 Abs, followed by coculturing with tumor cells. Cocultures of sialidase-treated tumor cells with the blocked NK cells revealed reduced IFNγ production (by 50%), whereas a 20% reduction was observed in cocultures with untreated tumor cells, compared with the IFN-γ production attained without blocking (Fig. 5*C*). Lysis of sialidase-treated cells cocultured with poly(I):poly(C)-induced spleen cells was reduced by 50–80% after NKG2D blocking; however, cocultures of untreated cells grown in the same conditions showed less significant lysis reduction after blocking (Fig. 5*D*). Finally, the involvement of NKG2D in lysis of sialidase-treated cells was studied in vivo by i.v. injection of the cells into mice pretreated with 200 μg anti-NKG2D mAbs. Lysis of sialidase-treated cells was significantly reduced in NKG2D-treated mice, as compared with their lysis in naive mice (Fig. 5*E*). Thus, IFN-γ production and cell lysis are regulated by the accessibility of NKG2D ligands for binding to the NKG2D receptor. Accordingly, reduced sialic acid levels promote IFN-γ production and cell lysis by encouraging the binding of NKG2D to the receptor on NK cells.

## Discussion

This study demonstrates that surface sialylation is an important element of the MCA-induced cancer-immunoediting process. Thus, the degree of sialylation of surface molecules is one of the parameters selected during immunoediting of the tumor cell repertoire during tumorigenesis, which shapes the intrinsic immunogenicity of the malignant cells and patters of their interactions with the host immune system. Specifically, low levels of sialic acid on tumor cells in mice with impaired immunoediting are associated with increased interactions of the malignant cells with effector cells of the host immune system, leading to malignant cell rejection

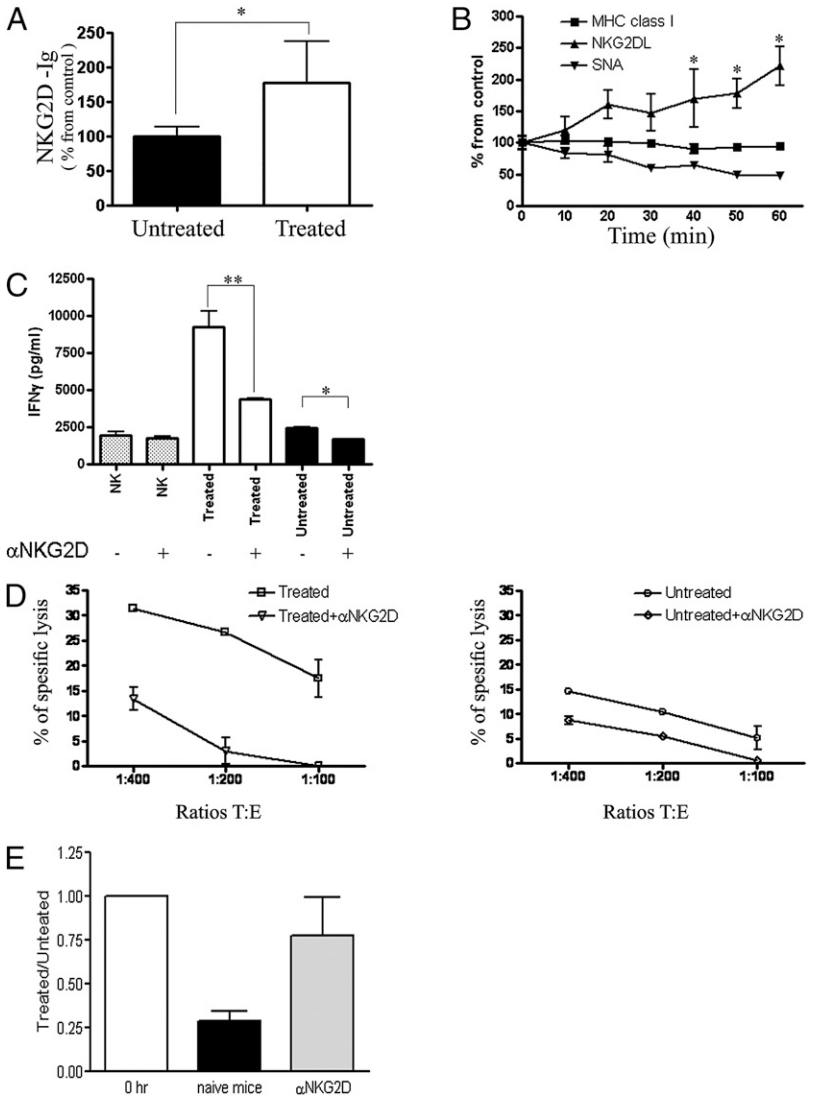


**FIGURE 5.** Sialylation is involved in the binding of NKG2D ligands and affects subsequent IFN-γ secretion and NK cell cytotoxicity. *A*, Four to five different MCA fibrosarcoma cell lines derived from WT mice were treated with sialidase, and binding of mNKG2D or mNCR1 fusion proteins was assessed. MCA fibrosarcoma cells derived from WT mice were treated with sialidase at 10 min intervals for 1 h to generate tumor cells bearing decreasing sialic acid levels on their surface. *B*, By using SNA lectin, anti–H-2K$^d$ Abs, or fmNKG2D, the sialic acid levels (▼), MHC class I presence (▲), or NKG2D ligand levels (■) were measured, respectively, and analyzed by flow cytometry. The binding values are presented as percentages, relative to the binding observed before sialidase treatment. *C*, Sialidase-treated or untreated cells were cocultured with activated NK cells or NKG2D-blocked NK cells, at a ratio of 1:1. NKG2D receptor blocking of the activated NK cells was observed by anti–NKG2D-CD134 Ab treatment; 24 h after coculturing these cells, IFN-γ secretion levels were measured in the supernatant by ELISA. *D*, Poly(I):poly(C) activated naive spleen cells labeled with CFSE were cocultured with sialidase-treated or untreated cells in the presence of anti–NKG2D-CD134 Abs (▽, ◊) or without these Abs (□, ○) at different target:effector ratios. *D*, After 5 h incubation at 37°C, cells were stained with 7-AAD, and specific lysis was calculated relative to the spontaneous lysis. *E*, Vybrant Dil-labeled sialidase-treated and Vybrant DiD-labeled untreated cells ($2 \times 10^7$) were mixed and injected into the tail veins of naive mice or mice preinjected with 200 μg anti–NKG2D-CD34 Abs. Lungs were harvested and cells were quantified 0 and 5 h after injection using flow cytometry. The ratio of treated target cells to untreated cells was calculated. Data represent the mean ± SD of duplicate or triplicate measurements from duplicate or triplicate independent experiments. $^{**}p < 0.01$; $^{*}p < 0.05$, versus the appropriate controls in each panel.

in intact mice. In mice with an intact immune system, the malignant cells that arise during MCA-induced carcinogenesis are enriched with surface sialic acid residues and are not eradicated by the immune responses. These observations were obtained when using MCA fibrosarcoma cell lines derived from IL-1α$^{-/-}$ (18, 19) and IFN-γ$^{-/-}$ mice (12, 20), in which impaired immunoediting has been observed. In the case of MCA-induced fibrosarcoma cells from IL-1α$^{-/-}$ mice, we detected lower expression of α2-6 sialyltransferase, compared with MCA-induced lines derived from WT mice, which corroborates the results of Avidan et al. (19). Our data suggest that sialylation of the tumor cell surface or sialylation of specific moieties determines the differential ability to stimulate different immune responses. It has to be elucidated whether these observations also hold for immunoediting of epithelial tumors. Experimental approaches to assess the creation of the immunogenic repertoire during epithelial carcinogenesis are rare and complicated and have not been approached appropriately.

The less sialylated membrane-bound glycoconjugates were mimicked in this study to assess their interaction with the host immune system, using sialidase-treated nonimmunogenic cells derived from MCA-induced WT mice. The major immune cell type, which was shown to interact best with sialidase-treated tumor cells, is the NK cell. Alterations in cancer cell sialylation have been correlated previously with changes in the activity of one or more of 20 different sialyltransferases (37) in malignant cells (4). Alterations in sialylation levels of malignant cells have usually been associated with changes in invasiveness and metastasis patterns, yet seldom related to the immunogenicity of the cells or their interaction patterns with immune effector cells. Concerning sialylated tumor cell interactions with immune effector cells, it was shown, for example, that sialylated GM2 gangliosides on YAC-1 lymphoma cells inhibit in vitro interactions with cytotoxic NK cells (38). The oversialylated T- and Tn-Ags of MUC1 in breast carcinoma cells simultaneously increased IL-10 and reduced IL-12 production by dendritic cells (39). The GD3 ganglioside on tumor cells, when enriched with disialic acids, inhibits cytotoxicity of NK cells via siglec-7 (40). High levels of gangliosides secreted by tumor cells inhibit the expression of costimulatory molecules on dendritic cells, subsequently reducing APC-dependent T cell proliferation (41). All these reports show that sialylated molecules expressed on or secreted by the malignant cells induce immune evasion by the malignant cells and their subsequent progression. Accordingly, reduction of tumor cell sialylation levels should lead to better antitumor immune responses, as observed in this study.

In this study, we have also shown the role of sialic acids on tumor cell killing activity, contact with NK cells, and IFN-γ secretion by NK cells. Thus, depletion experiments confirmed the

involvement of NK cell-mediated in in vivo growth inhibition of desialylated tumors. The increase in the number of immune synapses formed between NK cells and sialidase-treated tumor cells demonstrated that their interactions are essential for lysis of malignant cells by NK cells. In addition, NK cells were shown to represent the major population that secretes augmented amounts of IFN-γ after interacting with sialidase-treated tumor cells in vitro. NK cell-derived IFN-γ may be involved in modulating innate and adaptive immune responses (42). For example, priming of Th1-biased T cell responses promotes the development of an antitumor $CD8^+$ T cell response (43) or can activate macrophages and possibly other effector cells, leading to enhanced tumoricidal activity (44). Depletion of $CD4^+$ or $CD8^+$ T cells did not shift growth patterns of sialidase-treated tumor cells, whereas NK cell depletion induced progressive growth. This finding implies that NK cells rather than adaptive immune cells possibly control the initial phase of tumor growth.

NKG2D has been shown to play a prominent role in the antitumor immune response (45) by coupling the NKG2D receptor to its ligands on tumor cells, which triggers NK cell cytolytic activity and IFN-γ secretion (46, 47). Our results show enhancement of NKG2D receptor–ligand interactions, but no alteration in the levels of MHC class I expression, upon removing sialic acids. NKG2D receptor–ligand interactions in the sialidase-treated tumor cells were correlated to enhanced secretion of IFN-γ and in vitro or in vivo killing capacity. Moreover, blocking NKG2D prevented the interactions with the sialidase-treated cells, thus decreasing the lysis of these tumor cells by the cytotoxic NK cells. We hypothesize that tumor cell sialylation prevents the interactions of NKG2D receptor ligands through nonspecific charge repulsion of sialic acid residues near the NKG2D ligands (48). Another possible option for preventing ligand–receptor interactions is sialylation of NKG2D ligands (49), which have several potential glycosylation sites on their backbones (accession nos. O08602, O08603, and O08604 SwissProt database: http://www.expasy.org/sprot/). However, O'Callaghan et al. (50) showed that NKG2D glycosylation is not necessary for the NKG2D–REA1 and NKG2D–H60 interactions. Further work is needed to demonstrate how sialylation affects NKG2D ligand function regarding NK cell cytotoxicity and, if so, which NKG2D ligand is affected by sialylation and by which mechanism.

In conclusion, a high degree of tumor cell sialylation is a factor that was selected in the process of immunoediting during carcinogenesis. Although the direct interactions of sialic acid residues with lectin receptors, such as siglecs on NK cells, can be a negative regulator of cytolytic responses, we focused on signals activating the immune system by low sialylated tumor cells. By reducing surface sialylation, we generated more immunogenic tumor cell variants, which activated innate immune cells. By in vivo and in vitro studies, NK cells were shown to participate in growth inhibition of tumors expressing low levels of sialic acid. Furthermore, NK cell activity and cytotoxicity, as well as NKG2D ligand-receptor engagement, were shown to be dependent on the expression of tumor surface sialic acids. Finally, NKG2D is a key receptor involved in the lysis of desialylated tumor cells. Based on these observations, we suggest that tumor sialylation plays a role in tumor immunoediting. Desialylation of malignant cells could thus serve as a future approach to induce immunogenic tumor cells in personalized medicine approaches to treat patients with cancer.

## Acknowledgments

We thank Rosalyn M. White and Rona Baron from the Microbiology and Immunology Department of Ben-Gurion University for technical assistance.

## Disclosures

The authors have no financial conflicts of interest.

## References

1. Varki, A. 2007. Glycan-based interactions involving vertebrate sialic-acid-recognizing proteins. *Nature* 446: 1023–1029.
2. Fuster, M. M., and J. D. Esko. 2005. The sweet and sour of cancer: glycans as novel therapeutic targets. *Nat. Rev. Cancer* 5: 526–542.
3. Hedlund, M., E. Ng, A. Varki, and N. M. Varki. 2008. alpha 2-6-Linked sialic acids on N-glycans modulate carcinoma differentiation in vivo. *Cancer Res.* 68: 388–394.
4. Varki, N. M., and A. Varki. 2007. Diversity in cell surface sialic acid presentations: implications for biology and disease. *Lab. Invest.* 87: 851–857.
5. Hakomori, S. 1996. Tumor malignancy defined by aberrant glycosylation and sphingo(glyco)lipid metabolism. *Cancer Res.* 56: 5309–5318.
6. Wölfl, M., W. Y. Batten, C. Posovszky, H. Bernhard, and F. Berthold. 2002. Gangliosides inhibit the development from monocytes to dendritic cells. *Clin. Exp. Immunol.* 130: 441–448.
7. Miyazaki, K., K. Ohmori, M. Izawa, T. Koike, K. Kumamoto, K. Furukawa, T. Ando, M. Kiso, T. Yamaji, Y. Hashimoto, et al. 2004. Loss of disialyl Lewis(a), the ligand for lymphocyte inhibitory receptor sialic acid-binding immunoglobulin-like lectin-7 (Siglec-7) associated with increased sialyl Lewis(a) expression on human colon cancers. *Cancer Res.* 64: 4498–4505.
8. von Gunten, S., and H. U. Simon. 2006. Sialic acid binding immunoglobulin-like lectins may regulate innate immune responses by modulating the life span of granulocytes. *FASEB J.* 20: 601–605.
9. Aarnoudse, C. A., J. J. Garcia Vallejo, E. Saeland, and Y. van Kooyk. 2006. Recognition of tumor glycans by antigen-presenting cells. *Curr. Opin. Immunol.* 18: 105–111.
10. Kopitz, J., C. von Reitzenstein, M. Burchert, M. Cantz, and H. J. Gabius. 1998. Galectin-1 is a major receptor for ganglioside GM1, a product of the growth-controlling activity of a cell surface ganglioside sialidase, on human neuroblastoma cells in culture. *J. Biol. Chem.* 273: 11205–11211.
11. van Kooyk, Y., and G. A. Rabinovich. 2008. Protein-glycan interactions in the control of innate and adaptive immune responses. *Nat. Immunol.* 9: 593–601.
12. Dunn, G. P., C. M. Koebel, and R. D. Schreiber. 2006. Interferons, immunity and cancer immunoediting. *Nat. Rev. Immunol.* 6: 836–848.
13. Dunn, G. P., L. J. Old, and R. D. Schreiber. 2004. The immunobiology of cancer immunosurveillance and immunoediting. *Immunity* 21: 137–148.
14. Shankaran, V., H. Ikeda, A. T. Bruce, J. M. White, P. E. Swanson, L. J. Old, and R. D. Schreiber. 2001. IFNgamma and lymphocytes prevent primary tumour development and shape tumour immunogenicity. *Nature* 410: 1107–1111.
15. Smyth, M. J., G. P. Dunn, and R. D. Schreiber. 2006. Cancer immunosurveillance and immunoediting: the roles of immunity in suppressing tumor development and shaping tumor immunogenicity. *Adv. Immunol.* 90: 1–50.
16. Dunn, G. P., L. J. Old, and R. D. Schreiber. 2004. The three Es of cancer immunoediting. *Annu. Rev. Immunol.* 22: 329–360.
17. Zitvogel, L., A. Tesniere, and G. Kroemer. 2006. Cancer despite immunosurveillance: immunoselection and immunosubversion. *Nat. Rev. Immunol.* 6: 715–727.
18. Elkabets, M., Y. Krelin, S. Dotan, A. Cerwenka, A. Porgador, R. G. Lichtenstein, M. R. White, M. Zoller, Y. Iwakura, C. A. Dinarello, et al. 2009. Host-derived interleukin-1alpha is important in determining the immunogenicity of 3-methylcholantrene tumor cells. *J. Immunol.* 182: 4874–4881.
19. Avidan, A., M. Perlmutter, S. Tal, O. Oraki, T. Kapp, Y. Krelin, M. Elkabets, S. Dotan, R. N. Apte, and R. G. Lichtenstein. 2009. Differences in the sialylation patterns of membrane stress proteins in chemical carcinogen-induced tumors developed in BALB/c and IL-1alpha deficient mice. *Glycoconj J.* 26: 1181–1195.
20. Street, S. E., E. Cretney, and M. J. Smyth. 2001. Perforin and interferon-gamma activities independently control tumor initiation, growth, and metastasis. *Blood* 97: 192–197.
21. Waldhauer, I., and A. Steinle. 2008. NK cells and cancer immunosurveillance. *Oncogene* 27: 5932–5943.
22. Lanier, L. L. 2008. Up on the tightrope: natural killer cell activation and inhibition. *Nat. Immunol.* 9: 495–502.
23. Raulet, D. H. 2003. Roles of the NKG2D immunoreceptor and its ligands. *Nat. Rev. Immunol.* 3: 781–790.
24. Bryceson, Y. T., M. E. March, H. G. Ljunggren, and E. O. Long. 2006. Synergy among receptors on resting NK cells for the activation of natural cytotoxicity and cytokine secretion. *Blood* 107: 159–166.
25. Jamieson, A. M., A. Diefenbach, C. W. McMahon, N. Xiong, J. R. Carlyle, and D. H. Raulet. 2002. The role of the NKG2D immunoreceptor in immune cell activation and natural killing. *Immunity* 17: 19–29.
26. Nausch, N., and A. Cerwenka. 2008. NKG2D ligands in tumor immunity. *Oncogene* 27: 5944–5958.
27. Horai, R., M. Asano, K. Sudo, H. Kanuka, M. Suzuki, M. Nishihara, M. Takahashi, and Y. Iwakura. 1998. Production of mice deficient in genes for interleukin (IL)-1alpha, IL-1beta, IL-1alpha/beta, and IL-1 receptor antagonist shows that IL-1beta is crucial in turpentine-induced fever development and glucocorticoid secretion. *J. Exp. Med.* 187: 1463–1475.
28. Krelin, Y., E. Voronov, S. Dotan, M. Elkabets, E. Reich, M. Fogel, M. Huszar, Y. Iwakura, S. Segal, C. A. Dinarello, and R. N. Apte. 2007. Interleukin-1beta-driven inflammation promotes the development and invasiveness of chemical carcinogen-induced tumors. *Cancer Res.* 67: 1062–1071.

29. Mahabeleshwar, G. H., P. R. Somanath, and T. V. Byzova. 2006. Methods for isolation of endothelial and smooth muscle cells and in vitro proliferation assays. *Methods Mol. Med.* 129: 197–208.
30. Kuczek, T., and D. E. Axelrod. 1987. Tumor cell heterogeneity: divided-colony assay for measuring drug response. *Proc. Natl. Acad. Sci. USA* 84: 4490–4494.
31. Cerwenka, A., A. B. Bakker, T. McClanahan, J. Wagner, J. Wu, J. H. Phillips, and L. L. Lanier. 2000. Retinoic acid early inducible genes define a ligand family for the activating NKG2D receptor in mice. *Immunity* 12: 721–727.
32. Mori, N., Y. Yamashita, T. Tsuzuki, A. Nakayama, M. Nakazawa, Y. Hasegawa, H. Kojima, and T. Nagasawa. 2000. Lymphomatous features of aggressive NK cell leukaemia/lymphoma with massive necrosis, haemophagocytosis and EB virus infection. *Histopathology* 37: 363–371.
33. Song, X., Y. Krelin, T. Dvorkin, O. Bjorkdahl, S. Segal, C. A. Dinarello, E. Voronov, and R. N. Apte. 2005. CD11b+/Gr-1+ immature myeloid cells mediate suppression of T cells in mice bearing tumors of IL-1beta-secreting cells. *J. Immunol.* 175: 8200–8208.
34. Gazit, R., R. Gruda, M. Elboim, T. I. Arnon, G. Katz, H. Achdout, J. Hanna, U. Qimron, G. Landau, E. Greenbaum, et al. 2006. Lethal influenza infection in the absence of the natural killer cell receptor gene Ncr1. *Nat. Immunol.* 7: 517–523.
35. Lecoeur, H., M. Février, S. Garcia, Y. Rivière, and M. L. Gougeon. 2001. A novel flow cytometric assay for quantitation and multiparametric characterization of cell-mediated cytotoxicity. *J. Immunol. Methods* 253: 177–187.
36. Gubbels, J. A., M. Felder, S. Horibata, J. A. Belisle, A. Kapur, H. Holden, S. Petrie, M. Migneault, C. Rancourt, J. P. Connor, and M. S. Patankar. 2010. MUC16 provides immune protection by inhibiting synapse formation between NK and ovarian tumor cells. *Mol. Cancer* 9: 11.
37. Dall'Olio, F., and M. Chiricolo. 2001. Sialyltransferases in cancer. *Glycoconj. J.* 18: 841–850.
38. Yogeeswaran, G., A. Gronberg, M. Hansson, T. Dalianis, R. Kiessling, and R. M. Welsh. 1981. Correlation of glycosphingolipids and sialic acid in YAC-1 lymphoma variants with their sensitivity to natural killer-cell-mediated lysis. *Int. J. Cancer* 28: 517–526.
39. Rughetti, A., I. Pellicciotta, M. Biffoni, M. Bäckström, T. Link, E. P. Bennet, H. Clausen, T. Noll, G. C. Hansson, J. M. Burchell, et al. 2005. Recombinant tumor-associated MUC1 glycoprotein impairs the differentiation and function of dendritic cells. *J. Immunol.* 174: 7764–7772.
40. Nicoll, G., T. Avril, K. Lock, K. Furukawa, N. Bovin, and P. R. Crocker. 2003. Ganglioside GD3 expression on target cells can modulate NK cell cytotoxicity via siglec-7-dependent and -independent mechanisms. *Eur. J. Immunol.* 33: 1642–1648.
41. Caldwell, S., A. Heitger, W. Shen, Y. Liu, B. Taylor, and S. Ladisch. 2003. Mechanisms of ganglioside inhibition of APC function. *J. Immunol.* 171: 1676–1683.
42. Andoniou, C. E., J. D. Coudert, and M. A. Degli-Esposti. 2008. Killers and beyond: NK-cell-mediated control of immune responses. *Eur. J. Immunol.* 38: 2938–2942.
43. Mocikat, R., H. Braumüller, A. Gumy, O. Egeter, H. Ziegler, U. Reusch, A. Bubeck, J. Louis, R. Mailhammer, G. Riethmüller, et al. 2003. Natural killer cells activated by MHC class I(low) targets prime dendritic cells to induce protective CD8 T cell responses. *Immunity* 19: 561–569.
44. Hori, K., E. Mihich, and M. J. Ehrke. 1989. Role of tumor necrosis factor and interleukin 1 in gamma-interferon-promoted activation of mouse tumoricidal macrophages. *Cancer Res.* 49: 2606–2614.
45. Guerra, N., Y. X. Tan, N. T. Joncker, A. Choy, F. Gallardo, N. Xiong, S. Knoblaugh, D. Cado, N. M. Greenberg, N. M. Greenberg, and D. H. Raulet. 2008. NKG2D-deficient mice are defective in tumor surveillance in models of spontaneous malignancy. *Immunity* 28: 571–580.
46. Hayakawa, Y., and M. J. Smyth. 2006. Innate immune recognition and suppression of tumors. *Adv. Cancer Res.* 95: 293–322.
47. Lanier, L. L. 2005. NKG2D in innate and adaptive immunity. *Adv. Exp. Med. Biol.* 560: 51–56.
48. Floutsis, G., L. Ulsh, and S. Ladisch. 1989. Immunosuppressive activity of human neuroblastoma tumor gangliosides. *Int. J. Cancer* 43: 6–9.
49. Imaizumi, Y., K. Higai, C. Suzuki, Y. Azuma, and K. Matsumoto. 2009. NKG2D and CD94 bind to multimeric alpha2,3-linked N-acetylneuraminic acid. *Biochem. Biophys. Res. Commun.* 382: 604–608.
50. O'Callaghan, C. A., A. Cerwenka, B. E. Willcox, L. L. Lanier, and P. J. Bjorkman. 2001. Molecular competition for NKG2D: H60 and RAE1 compete unequally for NKG2D with dominance of H60. *Immunity* 15: 201–211.